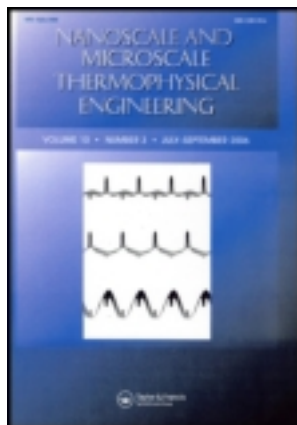


This article was downloaded by: [University of Virginia, Charlottesville]

On: 28 December 2012, At: 14:07

Publisher: Taylor & Francis

Informa Ltd Registered in England and Wales Registered Number: 1072954 Registered office: Mortimer House, 37-41 Mortimer Street, London W1T 3JH, UK



Microscale Thermophysical Engineering

Publication details, including instructions for authors and subscription information:

<http://www.tandfonline.com/loi/umte19>

Thin Film Non-Noble Transition Metal Thermophysical Properties

Andrew P. Caffrey^a, Patrick E. Hopkins^a, J. Michael Klopf^a & Pamela M. Norris^a

^a Department of Mechanical and Aerospace Engineering, University of Virginia, Charlottesville, Virginia, USA

Version of record first published: 16 Aug 2006.

To cite this article: Andrew P. Caffrey, Patrick E. Hopkins, J. Michael Klopf & Pamela M. Norris (2005): Thin Film Non-Noble Transition Metal Thermophysical Properties, *Microscale Thermophysical Engineering*, 9:4, 365-377

To link to this article: <http://dx.doi.org/10.1080/10893950500357970>

PLEASE SCROLL DOWN FOR ARTICLE

Full terms and conditions of use: <http://www.tandfonline.com/page/terms-and-conditions>

This article may be used for research, teaching, and private study purposes. Any substantial or systematic reproduction, redistribution, reselling, loan, sub-licensing, systematic supply, or distribution in any form to anyone is expressly forbidden.

The publisher does not give any warranty express or implied or make any representation that the contents will be complete or accurate or up to date. The accuracy of any instructions, formulae, and drug doses should be independently verified with primary sources. The publisher shall not be liable for any loss, actions, claims, proceedings, demand, or costs or damages whatsoever or howsoever caused arising directly or indirectly in connection with or arising out of the use of this material.

THIN FILM NON-NOBLE TRANSITION METAL THERMOPHYSICAL PROPERTIES

*Andrew P. Caffrey, Patrick E. Hopkins, J. Michael Klopff, and
Pamela M. Norris*

*Department of Mechanical and Aerospace Engineering, University of Virginia,
Charlottesville, Virginia, USA*

The transient thermoreflectance (TTR) technique coupled with a pump-probe experimental setup enables the observation of thermal transport phenomena on a sub-picosecond time scale. The reflectance from non-noble transition metals (at least one unoccupied d-orbital in the conduction band) can be shown to have a linear dependence when compared to small changes in the electron and lattice temperatures. This thermal dependence can be combined with the parabolic two step (PTS) model to enable measurement of the electron-phonon coupling factor and thermal conductivity of thin film materials. Experimental results are presented for thin film samples of the non-noble transition metals platinum and nickel. Results are presented using laser wavelengths ranging from 740 nm to 805 nm and using a range of laser fluences (ranging from ~ 0.35 to 2 J/m^2). Over this range of wavelengths and fluences the material properties are shown to be independent of the measurement conditions.

Keywords electron-phonon coupling, thermal conductivity, nickel, platinum, femtosecond, thin film, reflectance

INTRODUCTION

Measurement of energy transport properties in thin film materials has progressively gained interest, with direct industrial applications in micro- and opto-electronics. The transient thermoreflectance (TTR) technique, using an ultrashort-pulsed laser in a pump-probe configuration, has been used to measure thermal diffusivity [1–3], sound velocity [2, 4], and the electron-phonon coupling factor [5–7] of various thin metallic films. This technique excites a nonequilibrium heating event while monitoring the thermoreflectance response. The magnitude and phase of this signal are both significant and combine to yield the change in reflectance of the surface as a function of time [8]. The change in reflectance is then related to the change in temperature using an appropriate thermoreflectance model [9, 10]. A linear thermoreflectance model can be assumed for relatively small changes in temperature. In the non-noble transition metals nickel and platinum, interband transitions occur at relatively small energies, resulting in small temperature changes which are

Received 28 May 2004; accepted 19 November 2004.

The authors are grateful to the National Science Foundation (CTS-9908372) for their financial support. Address correspondence to Pamela Norris, Department of Mechanical and Aerospace Engineering, University of Virginia, 122 Engineer's Way, P.O. Box 400746, Charlottesville, VA 22904-4746, USA. E-mail: pamela@virginia.edu

NOMENCLATURE

<p><i>a</i> constant coefficient electron temperature, K^{-1}</p> <p><i>b</i> constant coefficient lattice temperature, K^{-1}</p> <p><i>C</i> heat capacity, $J/m^3 K$</p> <p><i>G</i> electron-phonon coupling factor, $W/m^3 K$</p> <p><i>J</i> fluence, J/m^2</p> <p><i>k</i> thermal conductivity, $W/m K$</p> <p><i>R</i> reflectivity</p> <p><i>S</i> laser source term, W/m^3</p> <p><i>T</i> temperature, K</p> <p><i>t</i> time, s</p> <p><i>x</i> direction normal to the sample surface</p>	<p>Greek Symbols</p> <p>γ heat capacity material parameter, $J/m^3 K^2$</p> <p>Δ change in</p> <p>δ optical penetration depth, nm</p> <p>λ laser wavelength, nm</p> <p>τ_p laser pulse width, fs</p> <p>Subscripts</p> <p><i>e</i> electron</p> <p>eq equilibrium</p> <p><i>l</i> phonon (lattice)</p> <p><i>o</i> room temperature</p>
--	--

easily determined from the linear thermorefectance model. Once the change in temperature of the sample surface is obtained, an accurate determination of the thermophysical properties is possible.

THERMAL MODEL

Energy transport through thin metallic films typically occurs on a picosecond time scale. Ultrashort-pulsed lasers are proven to be effective tools for monitoring energy transport with sub-picosecond temporal resolution. The ultrashort pulses are essential for the temporal resolution, while simultaneously inducing nonequilibrium heating. The rate of energy deposition is so rapid that there exists a brief period following the pulsed heating event when the electrons and lattice are not in thermal equilibrium. This nonequilibrium heating must be accounted for in the model for energy deposition and transport [11]. In 1974, Anisimov presented a two-temperature model for the laser heating of metals, which assumes that separate temperatures, T_e and T_l , can be defined to describe the local electron and lattice (phonon) temperature systems [11]. This model was later renamed the parabolic two step (PTS) model, since the electrons initially absorb the radiant energy, which is then transferred to the lattice as a second step [12]. Kaganov et al. originally derived the rate of energy exchange from collisions between electrons and phonons [13]. This rate is governed by a material property named the electron-phonon coupling factor, G , assumed to be constant at temperatures greater than the Debye temperature. The electrons diffusively transfer the energy throughout the thin metallic film at a rate determined by the thermal conductivity, consistent with Fourier's law, and in thin metallic films this process occurs over hundreds of picoseconds. These material properties represent the main mechanisms of energy transport in thin metallic films, and can be described by a complete thermal model.

The parabolic two step (PTS) model is comprised of two conservation of energy equations; one for the electrons absorbing the radiant energy, and a second equation describing the lattice contribution, Eqs. (1)–(2). In metals, the energy transport by free electrons is much greater than that by lattice vibrations, consistent with free electrons

being the primary energy carriers [14]

$$C_e(T_e) \frac{\partial T_e}{\partial t} = \frac{\partial}{\partial x} \left[k_e(T_e, T_l) \frac{\partial T_e}{\partial x} \right] - G(T_e - T_l) + S(x, t) \quad (1)$$

$$C_l \frac{\partial T_l}{\partial t} = G(T_e - T_l). \quad (2)$$

Since deviations in lattice temperature are minimal, the lattice heat capacity, C_l , is assumed constant. Temperature-dependent material properties include the electron heat capacity, C_e , and the electron thermal conductivity, k_e . The electron heat capacity is linearly related to the electron temperature in Eq. (3).

$$C_e(T_e) = \gamma T_e \quad (3)$$

The electron heat capacity constant, γ , can be determined empirically [15]. The temperature dependence of the electron thermal conductivity during nonequilibrium heating is proportional to the ratio of the electron and lattice temperatures:

$$k_e(T_e, T_l) = k_{\text{eq}}(T_o) \frac{T_e}{T_l} \quad (4)$$

The constant of proportionality in Eq. (4) is given by the equilibrium thermal conductivity, k_{eq} , which is measured at room temperature.

The laser source term, $S(x, t)$, in Eq. (1) has an exponential decay in space to account for absorption in a non-transparent medium, and a Gaussian shape in time, which gives a reasonable approximation of the laser pulse profile, as described by Eq. (5).

$$S(x, t) = 0.94 \frac{(1 - R)}{\tau_p \delta} J \exp \left[-\frac{x}{\delta} - 2.77 \left(\frac{t}{\tau_p} \right)^2 \right] \quad (5)$$

Properties of the material include the reflectivity, R , and the optical penetration depth, δ , while the fluence, J , and the pulse width, τ_p , are parameters of the incident laser pulse. This source term neglects any interaction with the substrate; therefore, the film must be thicker than the radiation penetration depth to ensure that the radiant energy does not reach the substrate. The Crank-Nicolson method is used with a nonuniform gridscheme to numerically solve Eqs. (1) and (2) by iterating the electron and lattice temperatures for each time step. After electron-phonon coupling, the thermal conductivity determines the rate of energy transfer for the next several hundred picoseconds. During this time, the ratio of the electron and lattice temperatures is approximately 1, causing the difference $T_e - T_l$ to be approximately zero. Consequently, the PTS model reduces to Fourier's law in this temporal range. With accurate numerical approximations of T_e and T_l , a theoretical PTS solution is calculated using thermophysical properties given in Table 1 [16].

Table 1. Properties for films used in PTS numerical calculations

Film material	Platinum	Nickel
Reflectance ($L = 29$ nm, Pt; $L = 22$ nm, Ni; $\theta_{inc} \approx 40^\circ$, R)	0.51	0.52
Reflectance ($L = 100$ nm; $\theta_{inc} \approx 40^\circ$, R)	0.54	0.55
Optical penetration depth, δ (nm)	13.5	14.3
Lattice heat capacity, C_l (J/m^3 K) [15]	2.85×10^6	3.95×10^6
Electron-phonon coupling factor (Si Substrate), G (W/m^3 K)	109×10^{16}	105×10^{16}
Electron heat capacity constant, γ (J/m^3 K ²) [15]	750	1064
Thermal conductivity, k_{bulk} (W/m K) [19]	71.6	90.7
Pulse duration, τ_p (fs)	190	190
Initial temperature, T_0 (K)	300	300

EXPERIMENTAL SETUP

The transient thermoreflectance (TTR) technique is used to measure the change in reflectance of the sample surface on a sub-picosecond time scale. A pump-probe experimental set-up employing a 76 MHz Ti:sapphire laser with an autocorrelated FWHM pulse width of ~ 190 fs is used for this investigation. A schematic of the experimental setup is shown in Figure 1 and the details and data acquisition procedure are described in the literature [11]. The laser used for this investigation enables an investigation over a limited tuning range of 1.4–1.7 eV (885–730 nm).

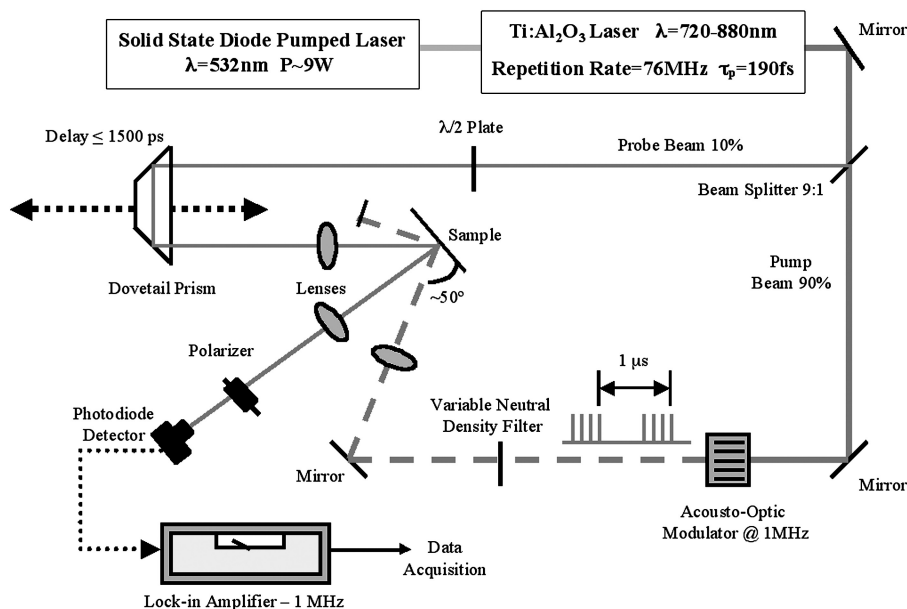


Figure 1. Experimental setup for the transient thermoreflectance (TTR) technique. For experimental details, please refer to [17].

THERMAL SENSOR

Recording data entails correlating the silicon photodiode voltage signal to a change in reflectance at the sample surface, as a function of experimental time. The signal amplitude, signal phase, and laser power are all incorporated to yield one dataset representing the true change in reflectance at the sample surface [8]. The signal phase is separable into transient and non-transient components. Although it is assumed that all the energy from the pump is dissipated prior to the arrival of the next pulse, the average power of the pump beam has been shown to cause slight residual heating in the film [8]. This heating is taken into account in the non-transient signal phase, leaving the transient component of the signal phase and the signal amplitude, from which can be determined the signal that arises due to the heating event. Recording the instantaneous laser power with each data point provides a reference of stability, since constant fluence is desired at the sample surface.

Properly determining thermophysical properties requires a correlation between changes in reflectance and temperature. It has been shown that the change in reflectance of a metallic surface can be directly related to the change in temperature [9]. When the incident probe photon energy approaches an interband transition energy, the reflectance becomes very sensitive. Rosei and Lynch presented a rough model for the change in the complex component of the dielectric function due to interband transitions [9]. Once the imaginary part of the dielectric function is known for all wavelengths, the Kramers-Kronig relationship can be used to calculate the unknown real part. An approximation of a linear relationship between reflectance and temperature, Eq. (6), is reasonable if changes in the electron temperature system do not exceed 100 K [10]:

$$\frac{\Delta R}{R} = a\Delta T_e + b\Delta T_l \quad (6)$$

Equation (6) provides an expression for comparing the experimental results to the PTS model, for determination of either the electron-phonon coupling factor or the thermal conductivity. Knowledge of both material properties is required in the PTS model. If the film thickness is comparable to the optical penetration depth of the material, it is called an optically thin film. By studying optically thin films, the electron-phonon coupling factor can be measured without precise knowledge of the thermal diffusivity because the film is heated volumetrically and the electron system quickly reaches thermal equilibrium. Once the electron-phonon coupling factor is known, the TTR technique can be used to measure the thermal conductivity normal to the sample surface in thicker films.

THERMOPHYSICAL PROPERTY MEASUREMENTS

The electron-phonon coupling factor has been measured for selected metals at room temperature, but there are many materials for which G is unknown [5, 7, 18]. Since G is a material constant, the value should be independent of the measurement technique, for any given sample. Electron beam evaporated samples of optically thin film platinum are deposited onto silicon wafers, coating an average film thickness of 29 nm (29 nm Pt/Si). The silicon substrates are 0.5 mm thick, with nominal n-type doping. The film

thickness is measured during evaporation by an in situ vibrating quartz crystal and then validated with a Tencor Alpha-Step 200 profilometer after deposition, measuring the actual thickness within ± 5 nm. Similar samples are created for 100 nm platinum, 22 nm nickel, and 100 nm nickel films, all on silicon substrates.

The optical penetration depths of the materials are a function of incident photon wavelength, λ , and the extinction coefficient, κ , which is the imaginary component of the index of refraction, as given by Eq. (7):

$$\delta = \frac{\lambda}{4\pi\kappa} \quad (7)$$

The optical penetration depths for Pt and Ni are reported in Table 1 averaged over the incident photon wavelengths in the working range of the laser. Laser wavelengths used on these optically thin samples are shown in Figures 2 and 3. The samples of Pt and Ni fabricated close to optical thickness of the respective materials ensure minimal thermal diffusion in the film when measuring electron-phonon coupling. The 100 nm samples of these metals allows for sufficient thermal diffusion to occur in the film before any interference by the substrate, allowing for accurate determination of the film thermal conductivity. The thermal diffusion time of these films is approximately 450 ps assuming bulk thermal diffusivity. By examining the thermal diffusion in the film in the first 200 ps, thermal conductivity can be accurately determined with minimal to no heating of the substrate.

By varying the incident laser power, the energy density reaching the sample surface can be controlled. As the incident fluence increases, the amount of energy deposited within the film increases, as demonstrated by the TTR data presented in Figure 4a. The largest fluence value relates to the largest change in reflectance, and the general shape of the decay in the response is similar for each of the plotted results. These TTR

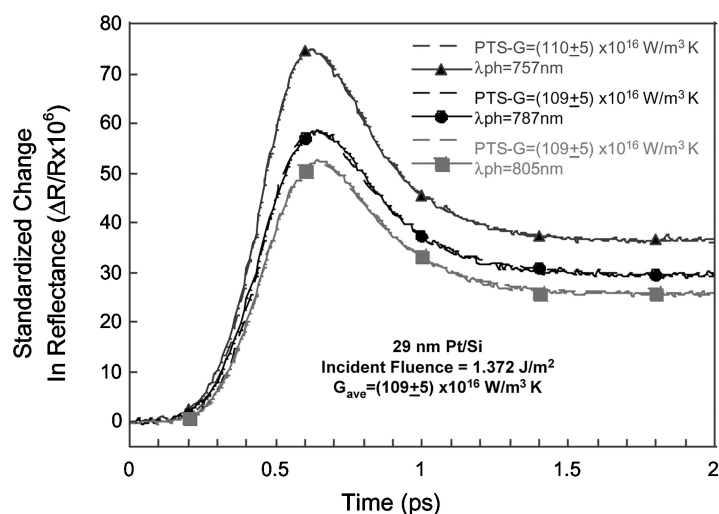


Figure 2. Electron-phonon coupling factor for a 29 nm Pt/Si sample, showing independence of measurement with incident photon wavelength.

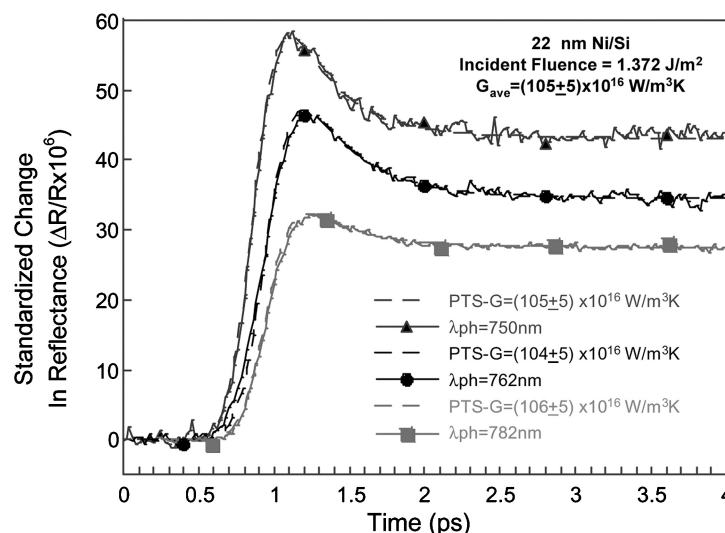


Figure 3. Electron-phonon coupling factor for a 22 nm Ni/Si sample, showing independence of measurement with incident photon wavelength.

data are numerically compared to the theoretical change in reflectance, Eqs. (1–6), to calculate a value for the electron-phonon coupling factor for Pt/Si, using values in Table 1. Each individual result is statistically verified by a least squares minimum, providing the best numerical solution to the PTS model [2]. The reported error is representative of the variation in redundant measurements, and is used to demonstrate reproducibility. All of the data sets were experimentally fit, determining the statistical mean of $G = (109 \pm 5) \times 10^{16} \text{ W/m}^3\text{K}$. Since the total number of measurements accumulated would be difficult to represent in each figure, it is accepted that the results are actually statistically sound, although each figure may appear to have only a small sample size.

To graphically represent the results of Figure 4a, the TTR data are re-expressed as demonstrated in Figure 4b. In this figure, the data are all normalized by the maximum value of the peak in the fast transient and superimposed. Although there is some random variation in the data evident (attributed to a scaling effect in the lowest fluence data) the curves are extremely similar in overall shape and rate of decay. Since the rate of decay of the response is related to G , the data qualitatively shows that the electron phonon coupling is constant despite different incident fluence. This idea of curve “shape” is similar to the methodology used to numerically fit TTR data to a PTS solution via a least-squares fitting routine [2]. Since the TTR data at different incident fluence values collectively normalize to nearly identical plots, the measured values of G are credible. This verifies that the measurement of the electron-phonon coupling factor is independent of incident fluence.

Figure 2 provides TTR data for varying photon wavelength, holding fluence constant, yielding a similar result to that of Figure 4a. Since all the incident photon energies considered are greater than the nearest interband transition energy in platinum ($\sim 0.6 \text{ eV}$), the linear model presented in Eq. (6) is appropriate throughout the tuning range [19].

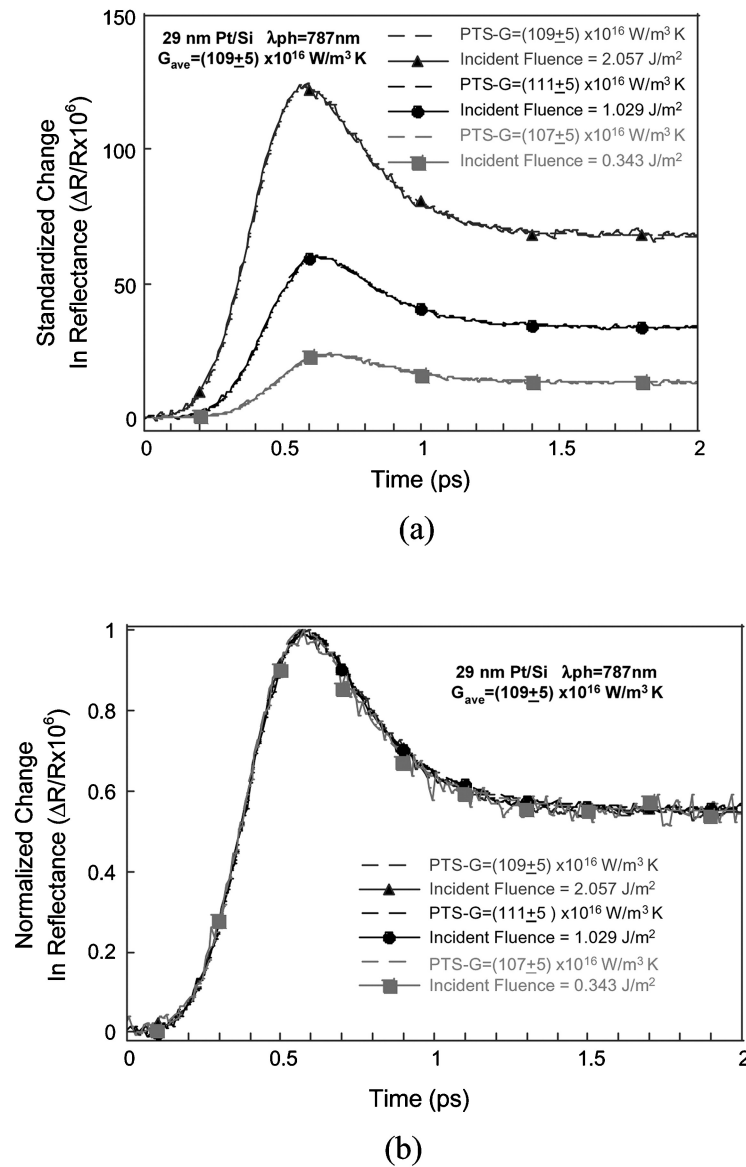


Figure 4. Electron-phonon coupling factor measurement for a 29 nm Pt/Si sample, (a) experimentally demonstrating independence of measurement with incident fluence, and (b) normalized at the peak of the fast transient, for visual verification of the measurement.

As the wavelength decreases, the photon energy increases, which corresponds with a larger change in reflectance signal. The general shape of each change in reflectance scan is similar among those plotted in Figure 2.

A similar measurement of G is performed using data provided in Figure 2 for constant fluence and varying wavelength. Once again, each of the scans in Figure 2 is

fit using the PTS model, and only a sample is presented for clarity. The electron-phonon coupling factor obtained by varying the photon wavelength is identical to that obtained previously found when incident pump fluence was varied. This result confirms that the value of $G = (109 \pm 5) \times 10^{16} \text{ W/m}^3\text{K}$ is a consistent measurement for platinum deposited on a silicon substrate. If the data in Figure 2 were normalized to the fast transient peak, the result would be very similar to Figure 4b. It should be no surprise that the electron-phonon coupling factor measured with this technique is truly independent of the wavelength of the laser light, but this is believed to be the first published experimental validation of this hypothesis.

As previously explained, once the value of G is determined, a measurement of thermal conductivity may be completed. As it was shown that the measured value of G is independent of the measurement technique, the thermal conductivity must be similarly investigated. Figure 5 provides a selection of TTR data acquired from a 100 nm Pt/Si thin metallic film, obtained by varying the incident pump fluence. The TTR data in Figure 5 have a time scale that is much larger than that for the measurement of the electron-phonon coupling factor in the previous figures. The PTS model deviates from the data in some regions of the scan. The curves overlay effectively between approximately 25 ps and 200 ps, except for the regions of 40–70 ps and 90–120 ps. As the electrons initially absorb the laser energy, the surface reflectance changes linearly, as indicated in Eq. (6). This rapid absorption of energy creates an isotropic stress in the film that generates an acoustic wave [20]. This wave propagates away from the surface, moving in all directions into the film. The acoustic wave that moves perpendicularly away from the sample surface will encounter the film-substrate interface and be partially reflected back to the film surface. Upon reaching the surface again, the change in reflectance is affected by this acoustic wave, which causes the “ripple” in data for the specified regions. The surface reflectance can be independently described as a function of temperature and strain effects, and is independent of the generated acoustic wave. These “echoes” can be ignored in the data, for the purpose of measuring thermal conductivity [20].

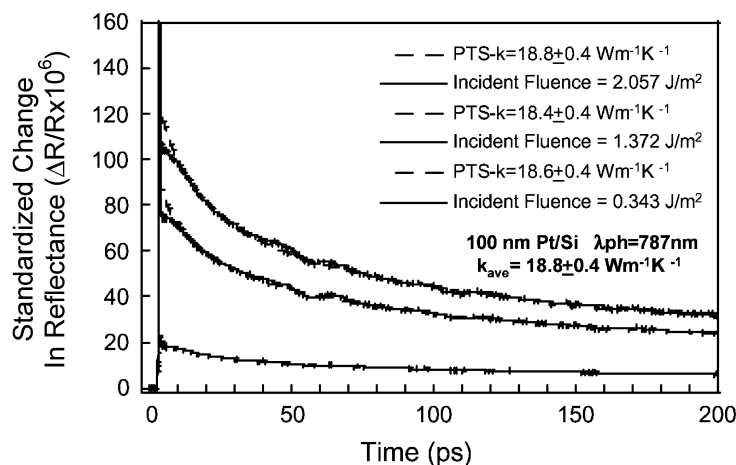


Figure 5. Thermal conductivity for a 100 nm Pt/Si sample, demonstrating independence of measurement with varying incident fluence.

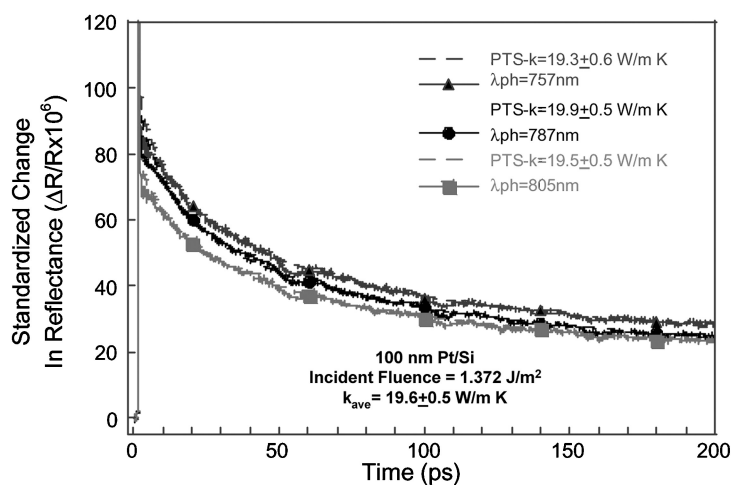


Figure 6. Thermal conductivity for a 100 nm Pt/Si sample, demonstrating independence of measurement with varying incident photon wavelength. Data were taken in a different location from Figure 5, yielding a different average value.

Unlike the electron-phonon coupling factor, it is understood that the thermal conductivity of thin film materials is often less than that of the corresponding bulk material. The measured value for the 100 nm Pt/Si sample is $k = 18.6 \pm 0.4$ W/mK, which is much less than the value for bulk platinum, $k = 71.6$ W/mK [21]. This deviation in k is attributed to the underlying microstructure, due to the presence of grain boundaries and interfaces [22]. Grains form during thin film deposition, and have a significant impact on energy transport within the film. Since thermal conductivity is dependent on thin film grains (and grain boundaries), it can be difficult to identify one k value as representative of the entire thin metallic film sample. Alternatively, the size of grains in electron beam evaporated films is usually larger than the respective electron and phonon mean free paths, so G is not affected by the film growth technique [22].

The data presented in Figure 6 are measured in a region of the thin film surface that is different from that measured in Figure 5. These data are acquired with varying photon wavelength, indicating that the measurement of k at a particular region in the film is independent of both the laser wavelength and fluence incident on the sample. This suggests each measurement is independently valid, and the thermal conductivity normal to the surface is highly non-constant throughout the film. To investigate this claim more fully, the data presented in Figure 7 are measured in different regions of the thin film surface, while holding the incident fluence and photon wavelength constant. The TTR datasets in Figure 7 are representative samples at each of the three locations, with multiple measurements determining error. If the thermal conductivity is constant throughout the film, these curves should overlay each other identically. There is some variation between the three curves, and the measured thermal conductivity normal to the surface is non-constant throughout the film. Since grains in electron-beam evaporated films are smaller than the focused spot size of the pump and probe beams, it is reasonable that some of the measurements are occurring with different grain boundary effects.

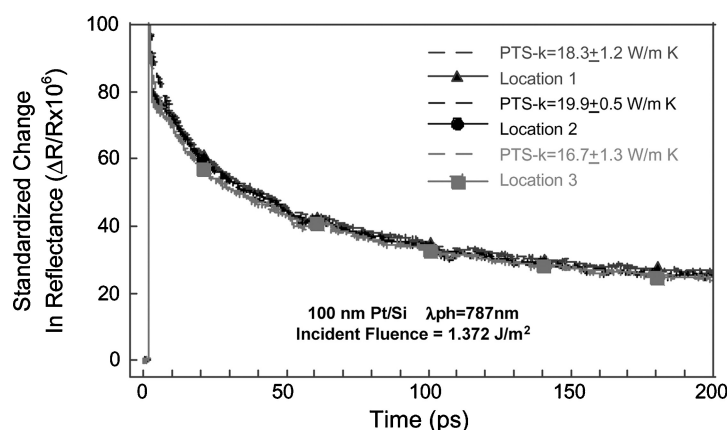


Figure 7. Results shown for a 100 nm Pt/Si sample, with each TTR scan taken in a different location of the thin film surface, showing variation of thermal conductivity with thin film structure.

As structural grains vary throughout the film, so does the thermal conductivity normal to the sample surface.

Electron beam evaporator systems are often used for creating thin metallic films used in microelectronics and opto-electronic devices. These results indicate that the overall heat transfer normal to the thin film is highly nonuniform, and dependent on film microstructure, which could have a major impact on device performance, and could ultimately lead to device failure. These results suggest performing similar thermal conductivity experimental measurements on thin film samples grown by other methods such as chemical vapor deposition (CVD) and molecular beam epitaxy (MBE) [23].

Results are presented for thin film nickel to verify that a second non-noble metal confirms the results obtained for platinum. As with platinum films, optically thin nickel films require the film thickness to be comparable to the optical penetration depth. An electron beam evaporated sample of nickel having a thickness of 22 nm is consistent with this argument, since the optical penetration depth is approximately 14 nm, as given in Table 1. In Figure 3, the electron-phonon coupling factor is measured for a large range of photon wavelengths, from which a small sample is presented. The interband transition energy of nickel (~ 0.5 eV) is far less than the chosen incident photon energies, so variation in photon wavelength will impact both interband and intraband transitions [24]. The experimental results are all extremely similar, within error, yielding a value of $G = (105 \pm 5) \times 10^{16}$ W/m³K for Ni/Si. Both nickel and platinum are non-noble transition metals that have similar electronic band and lattice structure, so obtaining similar results for G is satisfactory.

This G value is used to calculate a PTS solution predicting the thermal conductivity normal to a 100 nm Ni/Si sample, given in Figure 8. The measured value of $k = 52.7 \pm 0.7$ W/mK is less than the bulk nickel value $k = 90.7$ W/mK [21]. Since thermal conductivity may vary throughout the film, results from only one location are presented, for brevity. The measurements provided are consistent, and conclude that the TTR technique is capable of measuring thermophysical properties of non-noble transition metal thin films.

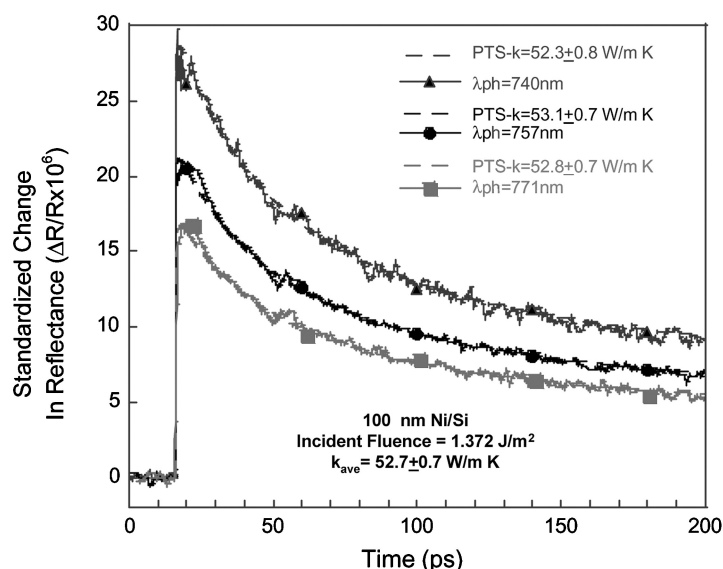


Figure 8. Thermal conductivity for a 100 nm Ni/Si sample, showing independence of measurement with incident photon wavelength.

CONCLUSIONS

Thermophysical property measurements have been presented for the non-noble transition metals platinum and nickel, as thin-films evaporated onto silicon substrates, over a range of laser wavelengths (740 to 805 nm) and using a range of laser fluences (ranging from ~ 0.35 to 2 J/m^2). Numerical solutions were used to analyze experimental data taken on optically thin film samples to determine the electron-phonon coupling factor of each material. Using these values allowed for consistent local measurements of the thermal conductivity of platinum and nickel thin films. Over the range of wavelengths and fluences investigated, the material properties determined using the pump-probe technique are shown to be independent of the measurement conditions.

REFERENCES

1. C. A. Paddock and G. L. Eesley, Transient Thermoreflectance from Thin Metal Films, *Journal of Applied Physics*, vol. 60, pp. 285–290, 1986.
2. J. L. Hostetler, A. N. Smith, and P. M. Norris, Thin Film Thermal Conductivity and Thickness Measurements Using Picosecond Ultrasonics, *Microscale Thermophysical Engineering*, vol. 1, pp. 237–244, 1997.
3. N. Taketoshi, T. Baba, and A. Ono, Observation of Heat Diffusion across Submicrometer Metal Thin Films Using a Picosecond Thermoreflectance Technique, *Japanese Journal of Applied Physics*, vol. 38, pp. L1268–L1271 1999.
4. H. T. Grahn, H. J. Maris, and J. Tauc, Picosecond Ultrasonics, *IEEE Journal of Quantum Electronics*, vol. 25, pp. 2562–2569, 1989.
5. S. D. Brorson, A. Kazeroonian, J. S. Moodera, D. W. Face, T. K. Cheng, E. P. Ippen, M. S. Dresselhaus, and G. Dresselhaus, Femtosecond Room-Temperature Measurement of the Electron-

- Phonon Coupling Constant λ in Metallic Superconductors, *Physics Review Letters*, vol. 64, pp. 2172–2175, 1990.
6. H. E. Elsayed-Ali, T. Juhasz, G. O. Smith, and W. E. Bron, Femtosecond Thermorefectivity and Thermotransmissivity of Polycrystalline and Single-Crystalline Gold Films, *Physics Review B*, vol. 43, pp. 4488–4491, 1991.
 7. J. L. Hostetler, A. N. Smith, and P. M. Norris, Measurement of the Electron-Phonon Coupling Factor Dependence on Film Thickness and Grain Size in Au, Cr, and Al, *Applied Optics*, vol. 38, pp. 3614–3620, 1999.
 8. A. N. Smith, A. P. Caffrey, J. M. Klopff, and P. M. Norris, Importance of Signal Phase on the Transient ThermoReflectance Response as a Thermal Sensor, *Proceedings of the 35th National Heat Transfer Conference*, ASME, New York, pp. NHTC01 11221 1–6.
 9. R. Rosei and D. W. Lynch, Thermomodulation Spectra of Al, Au, and Cu, *Physics Review B*, vol. 5, pp. 3883–3394, 1972.
 10. S. D. Brorson, Femtosecond Room-Temperature Measurement of the Electron-Phonon Coupling Constant λ in Metallic Superconductors, *Physical Review Letters*, vol. 64, pp. 2172–2175, 1990.
 11. S. I. Anisimov, B. L. Kapeliovich and T. L. Perel'man, Electron Emission from Metal Surfaces Exposed to Ultrashort Laser Pulses, *Soviet Physics JETP*, vol. 39, pp. 375–377, 1974.
 12. T. Q. Qiu and C. L. Tien, Femtosecond Laser Heating of Multi-Layer Metals—I. Analysis, *International Journal of Heat and Mass Transfer*, vol. 37, pp. 2789–2797, 1994.
 13. M. I. Kaganov, I. M. Lifshitz, and L. V. Tanatarov, Relaxation between Electrons and the Crystalline Lattice, *Soviet Physics JETP*, vol. 4, pp. 173–178, 1957.
 14. T. Q. Qiu and C. L. Tien, Heat Transfer Mechanisms During Short-Pulsed Laser Heating of Metals, *Journal of Heat Transfer*, vol. 115, pp. 835–841, 1993.
 15. C. Kittel, *Introduction to Solid State Physics*, John Wiley & Sons, New York, 1995.
 16. A. N. Smith, J. L. Hostetler, and P. M. Norris, Nonequilibrium Heating in Metal Films: An Analytical and Numerical Analysis, *Numerical Heat Transfer A*, vol. 35, pp. 859–873, 1999.
 17. P. M. Norris, A. P. Caffrey, R. Stevens, J. M. Klopff, J. T. McLeskey, and A. N. Smith, Femtosecond Pump-Probe Nondestructive Evaluation of Materials, *Review of Scientific Instruments*, vol. 74, pp. 400–406, 2003.
 18. R. H. M. Groeneveld, R. Sprik, and A. Lagendijk, Ultrafast Relaxation of Electrons Probed by Surface Plasmons at a Thin Silver Film, *Physical Review Letters*, vol. 64, pp. 784–787, 1990.
 19. J. H. Weaver, Optical Properties of Rh, Pd, Ir, and Pt, *Physical Review B*, vol. 12, pp. 469–476, 1975.
 20. J. L. Hostetler, A. N. Smith, and P. M. Norris, Simultaneous Measurement of Thermophysical and Mechanical Properties of Thin Films, *International Journal of Thermophysics*, vol. 19, pp. 569–577, 1998.
 21. F. P. Incropera and D. P. DeWitt, *Fundamentals of Heat and Mass Transfer*, John Wiley & Sons, New York, 1996.
 22. D. G. Cahill, Heat Transport in Dielectric Thin Films and at Solid-Solid Interfaces, in C. L. Tien, A. Majumdar and F. M. Gerner (eds.), *Microscale Energy Transport*, Taylor & Francis, Washington, DC, 1998.
 23. J. L. Vossen and W. Kern, *Thin Film Processes II*, Academic Press, Boston, 1991.
 24. D. W. Lynch and W. R. Hunter, Comments on the Optical Constants of Metals and an Introduction to the Data for Several Metals, in E. D. Palik (ed.), *Handbook of Optical Constants of Solids*, Academic Press, Orlando, FL, 1985.